0273-2289/93/4201—0053$03.80

An Inexpensive Optical Probe for Measuring the Local Specific Interfacial Area

JENG-DAR YANG AND NAM SUN WANG*

Department of Chemical Engineering, University of Maryland, College Park, MD 20742

Received November 5, 1992; Accepted January 29, 1993

ABSTRACT

An *in situ* optical probe was developed to measure reliably the local specific interfacial area of the suspended phase (specifically air bubbles) in a bioreactor. The light transmission-based probe can be simply and inexpensively constructed from readily available components. The probe's performance was tested in a suspension of opaque monodisperse polystyrene spheres as well as in the presence of nonspherical, nonuniformly distributed bubbles. The probe signal is directly related to the local specific interfacial area by a calibration equation obtained with polystyrene beads, as opposed to the cumbersome direct photographic bubble measurements that the probe attempts to replace. Its utility was demonstrated by measuring the specific bubble interfacial area at two locations in a bioreactor at various agitation intensities.

Index Entries: Specific interfacial area; Sauter mean diameter; bubble measurement; gas holdup; optical probe; optical sensor; oxygen mass transfer coefficient; dispersed phase.

NOMENCLATURE

- a specific interfacial area of the suspended phase (surface area/total volume) (m^{-1})
- a' specific interfacial area of the suspended phase (surface area/medium volume) (m^{-1})

*Author to whom all correspondence and reprint requests should be addressed.

C constant
D_e equivalent spherical bubble diameter (m)
$D_{e,j}$ equivalent spherical diameter of the jth bubble (m)
D_{32} Sauter mean diameter of the suspended phase (m)
f correction factor defined as $(V_s - V_0)/(V_s - V)$
I light intensity after the introduction of the dispersed phase (photons/m^2–s)
I_0 light intensity before the introduction of the dispersed phase (photons/m^2–s)
K mie scattering factor
l light path length (m)
l_H the length of the major axis of an ellipsoid bubble (m)
l_v the length of the minor axis of an ellipsoid bubble (m)
m functional constant of photoresistor
N total number of bubbles
n functional constant of photoresistor
R photoresistor's resistance (ohm)
V voltage reading after the introduction of the dispersed phase (volt)
V_0 voltage reading before the introduction of the dispersed phase (volt)
V_s circuit driving voltage (volt)
ϕ holdup of the suspended phase

INTRODUCTION

The specific interfacial area a is defined as the surface area of the suspended phase per total volume. Note that the interfacial area per medium volume a', is also commonly used. These two quantities differ by the holdup of the dispersed phase, ϕ.

$$a = a'(1 - \phi) \tag{1}$$

The specific interfacial area is a crucial design parameter in mass-transfer operations involving immiscible two-phase systems containing gas bubbles, solid particles, or liquid droplets. As a result of the spatial inhomogeneity within a mixing tank, a is generally a function of the speciic location. The industrial demand for the measurement of a is well established in a wide range of fields. In bioprocess engineering in particular, the importance of this parameter is reflected in the extensive effort in maintaining the specific bubble interfacial area for oxygen mass transfer in scaling up a bioreactor. Knowledge of the local bubble interfacial area in a bioreactor is critical in evaluating the extent of mixing and mass transfer across the interface—properties that depend on the stirrer type and baffle/sparger location. For example, the overall oxygen mass transfer coefficient in a bioreactor is a product of the oxygen transfer coefficient k_l and the volume-averaged interfacial area per medium volume $\bar{a}'$. Experimentally, the combined product of $k_l\bar{a}'$ is esimated either dynamically with a dissolved

oxygen probe or statically via chemical sulfite oxidation, but the individual terms are seldom reported because they are much more difficult to measure. Reports on the local values of a are even rarer.

Many methods exist for measuring a. Jones and Delhaye (*1*) and Ishii (*2*) give comprehensive reviews on various methods. The most direct way of measuring a perhaps is by physical means. Given the local gas holdup, ϕ, and the time-averaged Sauter mean diameter, D_{32}, of the suspended phase at the same location, the local value of a is determined via the following relationship:

$$a = 6\phi / D_{32} \tag{2}$$

Note that the above equation and its subsequent use throughout the manuscript consistently refer to the local value, not volume-averaged over the entire bioreactor. The local holdup ϕ in the above equation can be measured, for example, with the device of Yang and Wang (*3*). The device withdraws the gas-liquid dispersion sample from aerated media at a superficial velocity that matches the local flow velocity (isokinetic sampling) and measures the individual volumes of gas and liquid after phase separation. The Sauter mean diameter of the suspended phase is often measured with the photographic method. Unless coupled to a completely automated digital image analysis system, the process of counting the number of bubbles and measuring the size of each individual bubble in a series of still photographs is tremendously tedious. Furthermore, the photographic method is not generally applicable to stainless steel vessels that are common in large scale fermentations. At best, it is restricted to only the relatively small region near the window where a camera can be mounted. Even for a clear glass vessel, it is restricted by the limited depth of field at each focal length. Consequently, the photographic measurement near the wall yield results that may not be representative of the rest of the bioreactor because of wall effects.

Alternatively, a can be measured based on light transmission. As the dispersed phase passes through a small gap between the light source and the photosensor, it simultaneously diffracts, refracts, absorbs, and reflects light projected from the light source, resulting in a reduction in the intensity of light being detected by the photosensor. Thus, the specific interfacial area can be determined from a reduction in transmitted light caused by the presence of bubbles, as well as droplets and particles. Because of this method's fast response, nondestructiveness, accuracy, and reproducibility, it is highly effective under certain medium conditions. These conditions will be elaborated later.

Several probes based on light transmission have been developed in the past, dating back more than three decades. The optical probe described by Vermeulen et al. (*4*) for the interfacial area measurement required information on the refractive indices of both the dispersed and continuous phases for interpreting the probe response. Calderbank (*5*) constructed a

probe in which the light source and the photosensor were both placed externally, and the light beam was guided into the mixing tank by a series of mirrors placed in an immersed tube. In addition, Calderbank derived a mathematical model to convert the response signal to the interfacial area. The model was later shown by McLaughlin and Rushton (*6*) to be equally applicable to dispersed phases of solids, liquids, and gases alike as long as the size of the dispersed phase remained larger than 0.1 mm, which is the range encountered in most practical applications. Their calibration equation was shown to be universally valid for both transparent and opaque as well as uniformly and nonuniformly shaped particles in the dispersed phase. Based on the same concept, Hong and Lee (*7*) created a light transmission probe by coupling optical fibers with a spectrophotometer.

More recent, refined methods include ultrasound (*8,9*). Despite the long history on the development of probes to measure a, it is emphasized that there remains a real need to measure the interfacial area of bubbles in a bioreactor (and other two-phase vessels). However, an affordable commercial product for such a purpose is unfortunately simply unavailable. The consequence is that a probe, possibly with inferior performance, must be custom-made at a considerable cost. It is this prohibitive cost that has kept the interfacial area measurement beyond the reach of most fermentation technologists. In this manuscript, we attempt to fill just such a void by developing an *inexpensive*, practical probe and the associated methodology for signal interpretation. Although the present probe's working principle is based on the same proven light transmission method as many past ones, which should be viewed as an advantage, it is significantly different from them in its physical design, stability, compactness, ease of fabrication, and practical utility.

In this work, the probe was first tested with monodisperse, opaque polystyrene spheres, then further analyzed with nonspherical, nonuniform-sized bubbles in an agitated medium in a bioreactor. Bubbles of different average sizes, thus different values of a, were generated by changing the agitation intensity. To obtain a gas dispersion with a higher value of a, a surface active chemical, sodium dodecyl sulfate (SDS, 4 ppm), was added to the medium. Finally, the measurement of a at various locations in a bioreactor is demonstrated with the probe. This article's discussion centers on air bubbles in a bioreactor in particular, but the results should generically carry over to the other types of suspended phases such as solid particles and immensible liquid droplets.

PROBE DEVELOPMENT

The schematic diagram of the device is shown in Fig. 1, and the probe's actual configuration and its relative dimension with respect to a 14-L bioreactor can be seen in Fig. 2. The device shown in Fig. 1 has a dimension

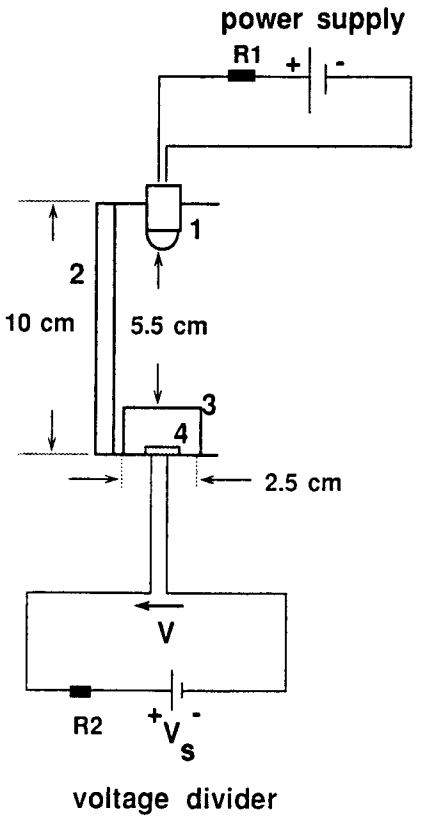

Fig. 1. Schematic diagram of the optical probe for measuring the specific interfacial area.

of 2.5 cm × 2.5 cm × 10 cm, or approx 50 cm^3. We have used the probe in a 1-L bioreactor and a 1-L flask alike without encountering any difficulty, which probably represent the lower limit on the bioreactor size. The probe is designed to provide sufficient accuracy and reasonable reproducibility for practical use. Some of the novel features that we find necessary to reduce cost and yet retain the probe's robustness after repeated experimentation are listed below. An inexpensive light emitting diode (LED) is chosen over an incandescent light bulb as the light source for its consistently narrow wavelength band and stable intensity. Although not critical, the LED's color can be selected to minimize the effect of possible changes in the medium's color intensity. Both the light source and the detector are placed directly in the medium, not outside the stirred vessel as are most other devices. The immersed electrical components are sealed against the medium with an epoxy resin. This immersed arrangement eliminates the

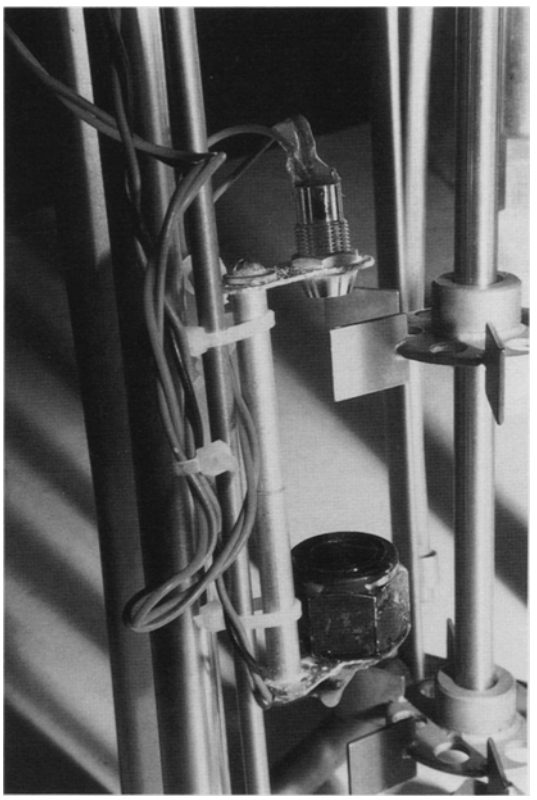

Fig. 2. A closeup view of the optical probe. The LED and the hood under which the photoresistor is housed are separated by an adjustable spacer. The stirrers and baffles extending from the fermentor headplate can be seen in the background.

need for light guiding devices/cables and reduces both light lost during transmission and the cost related to the extra devices. In addition, being miniature and lightweight, the probe can be easily placed at the desired location inside a vessel with only a minimal disturbance on the flow field. Thus, a more representative measurement of a can be achieved than the previous optical devices. Finally, consisting of only readily available components, the probe can be fabricated without an extensive development effort and is highly affordable (less than ten dollars for materials).

As indicated earlier, the working principle of this probe is based on light transmission. Green light from an LED (Radio Shack, #276-025) passes through the medium and impinges on a passive CdS photoresistor (Radio Shack, #276-118), whose electrical resistance R changes inversely with the light intensity I according to the following empirical constitutive equation:

$$R^n I = m \tag{3}$$

where m and n are the photoresistor constants. The photoresistor may be replaced by other common types of light sensors, e.g., photocells and phototransistors, without adversely affecting the probe's general utility. The photoresistor is sealed inside a hood and is recessed from the opening that is covered with a sheet of optically transparent glass. A light hood whose inner wall is painted black effectively absorbs stray light not in line with the light source. The separation between the light source and the detector, hence the light path length, can be adjusted to maximize the signal-to-noise ratio and extend the useful range of the probe.

By comparing the light intensities before and after the introduction of the dispersed phase, I_0 and I, respectively, the specific interfacial area of the dispersion is determined from the following relationship (*5*):

$$\log (I / I_0) = (Kl / 9.2)a \tag{4}$$

where K is the mie scattering factor, and l is the light path length. For the simple voltage divider circuit shown in Fig. 1, the above equation can be rewritten in terms of the photoresistor's response.

$$\log [(V / V_0)f] = (Kl / 9.2n)a = C \cdot a \tag{5}$$

where V_0 and V are the voltage readings before and after the introduction of the dispersed phase. The factor f, which is $(V_s - V_0)/(V_s - V)$, with V_s being the driving voltage, accounts for the nonlinearity of the circuit. Although not critical, alternative circuits can be designed to eliminate this nonlinearity (*10*). The validity of the above equation was first checked in a well-defined suspension of spherical polystyrene beads then further verified in bubble swarms in an agitated medium.

MATERIALS AND METHODS

Probe Testing with Spherical Polystyrene Beads

Two different sized (0.635 cm and 0.3175 cm) opaque spherical polystyrene beads with a special surface finish (Precision Plastic Ball, Chicago, IL) were suspended in a 1-L beaker containing a continuously agitated medium. The medium formula was the same as that used in our previous work (*3*). Because the number of beads required for a given surface area was rather large, the beads were weighed instead of being individually counted. The optical probe was placed in the optically sealed beaker, and the whole apparatus was maintained at 30°C in a water bath. The voltage signal was recorded by a personal computer equipped with an A/D converter (Data Translation, DT2801).

Probe Testing with Bubbles

Experiments with bubbles were conducted in a 14-L, cylindrical, flat-bottomed fermenter (New Brunswick, MF-114) which was baffled and equipped with two 6-bladed Rushton turbines. The dimensions of the fermentor and stirrers had been previously reported (3). The fermentor was filled with 10 L of the medium and controlled at 30°C. Through a sparger positioned underneath the stirrers, a constant air flow rate was maintained at 0.38 SLPM with a mass flow controller (Brooks, Model 5850E), which was volumetrically calibrated. The stirrer speed was calibrated with a stroboscope (General Radio, Model 1531-AB). Probe testing was conducted completely in the dark.

Determination of the Sauter Mean Diameter of Bubbles

The bubble diameter at the same spot covered by the optical probe was measured by the photographic method. Except for minor modifications, the macrophotographic (high magnification photography) system and the computerized image processing facility were similar to those of Chang (*11*). In this work, a camera (Nikon, F3) equipped with a 135 mm f/2.8 lens, an extension bellow, a motor drive, and a remote trigger release was mounted on a tripod. The shutter speed and the lens aperture were set at 1/125 s and f4.0, respectively. The bellow was extended to 13.5 cm to achieve a magnification ratio of 1.0 with a reduced depth of field. At this setting, the subject field covered 1.8 cm × 1.2 cm, and the distance between the front edge of the lens barrel and the focused subject was ~ 28.0 cm. To serve as the reference scale, a wire with a known diameter was placed on the same focal plane and photographed without agitation and sparging. Photographic frames taken consecutively in time covered only a small volume; thus, the value of D_{32} reported subsequently is an average over time at the same spatial point, not an average over the entire bioreactor volume. A thyristor flash (Sunpak, Model 611), set at 1/128 of its full power with a flash duration of ~ 1/50000 s, froze the bubble motion. The flash light was positioned at the opposing side of the fermentor to avoid reflection from the glass fermentor vessel. For bubble dispersions in the presence of SDS, the flash intensity and the lens aperture were adjusted at each agitation speed to obtain proper exposures. The exposed negatives were developed by following the directions accompanying the films (Kodak, Technical pan 2415).

A film strip projector (Dukane-500) displayed the negative bubble image on a wall-mounted digitizing pad (Didi-Pad, Model DP5A-2436L), which was equipped with a 16-button cursor and communicated to a personal computer via an RS232C serial connection at a 1200 baud rate. The

Fig. 3. A photograph showing some typical nonspherical bubbles in an agitated medium.

digitizing pad transmitted data in the ASCII format and had a resolution of 0.0025 cm and an accuracy of 0.025 cm. A typical photograph of bubbles in an agitated medium shown in Fig. 3 indicate that the irregular bubble shapes can be approximated by an ellipsoid. The lengths of the major axis and the minor axis, l_H and l_V, respectively, were estimated from the corresponding coordinates. These measurements, in turn, were used to estimate the equivalent spherical bubble diameter, D_e.

$$D_e = \sqrt[3]{(l_H\, l_V^2)} \tag{6}$$

Finally, the Sauter mean diameter of bubbles was calculated as:

$$D_{32} = (\Sigma_{j=1}^{N} D_{e,j}^3) \,/\, (\Sigma_{j=1}^{N} D_{e,j}^2) \tag{7}$$

where $D_{e,j}$ is the equivalent spherical diameter of the jth bubble, and N is the total number of bubbles considered. In determining the Sauter mean diameter, at least 300 bubbles were measured. Chen and Middleman (*12*) also recommended this number for determining the drop size distribution.

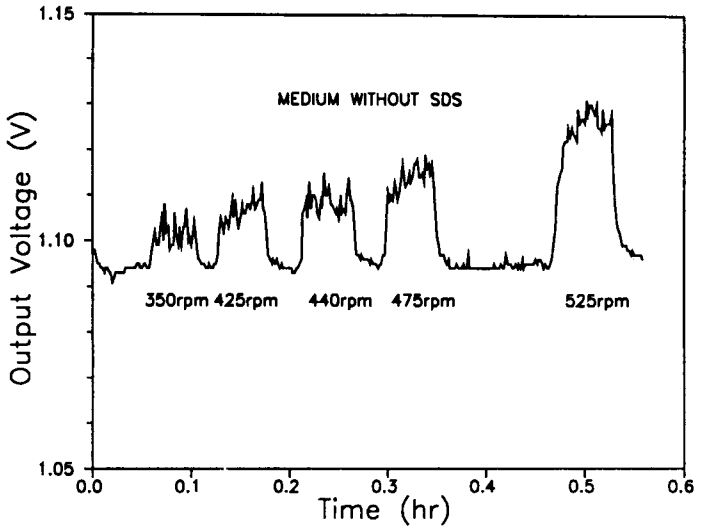

Fig. 4. Transient voltage response of the optical probe when subjected to aeration and agitation.

RESULTS AND DISCUSSION

The response of the probe at various agitation intensities with and without sparging are shown in Figure 4. The baseline represents the probe output in the absence of sparging. Immediately following the introduction of sparging, the output signal increased, and this increase became more significant as the agitation intensity increased. The signal fluctuation, as a direct result of the unavoidable discontinuous passage of bubbles in the light path, can be easily reduced by an averaging or noise filtering procedure. As demonstrated by the sharpness of the signal response to the on-off switching of the sparging, the probe displayed a rapid, instantaneous response to the dispersed phase. In addition, as demonstrated by the consistent baseline to which the signal returned after air sparging was turned off, the probe showed a negligible signal drift. The small visible downward transient toward the baseline was not caused by the probe's response but was indicative of the presence of residual air bubbles that continued to recirculate in the fermentor and did not surface immediately after sparging ws turned off. The long term stability of the baseline and the baseline's noise level were reasonable.

The probe was calibrated with uniformly sized polystyrene beads and bubbles. In the first case, calibration with polystyrene beads were performed in a beaker as described in the preceeding section. In the second case, a was calculated based on Eq. (2), where D_{32} was measured with the photographic method and ϕ was measured according to Yang and Wang (3). Both measurements of D_{32} and ϕ were taken at the same location as

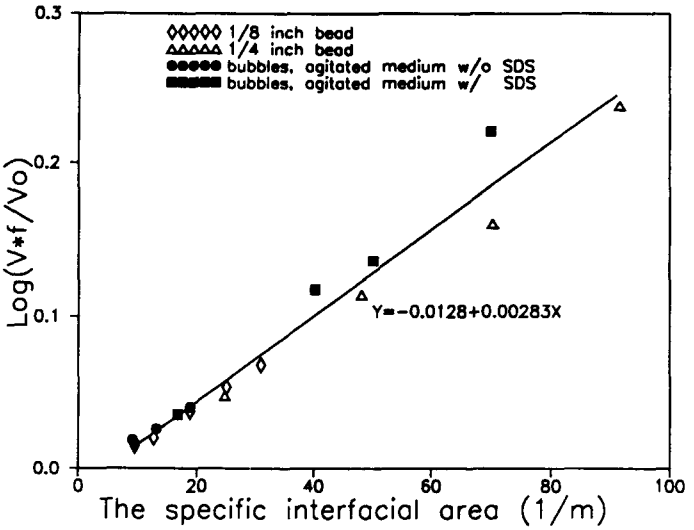

Fig. 5. Logarithmic voltage response of the optical probe as a function of the specific interfacial area. Based on this calibration curve, voltage readings can be readily converted to specific interfacial areas.

the optical probe, which was situated between the outer edge of the stirrer blades and the bioreactor vessel wall. In the entire agitation range under study, the Sauter mean diameter of bubbles was 0.13 ~ 0.16 cm in the absence of SDS and 0.06 ~ 0.11 cm in the presence of SDS. In Fig. 5, experimental data from both cases are correlated with the same straight line as predicted by Eq. (5). Thus, the single calibration line in Fig. 5 implies that the probe can be calibrated with polystyrene beads alone without resorting to the much more tedious photographic method, whose avoidance has motivated the development of the present optical probe in the first place.

A closer inspection of Fig. 5 reveals that most of the bead data lie slightly below the calibration line, but most of the bubble data lie slightly above it, with the discrepancy becoming more pronounced, albeit still tolerable, at higher values of a. This may be caused by the very different ways by which a was generated. In the bead method, a was raised by simply adding more beads (0.635 cm). On the other hand, the high interfacial area of bubbles was achieved by changing the agitation intensity and by adding SDS such that smaller bubbles (~ 0.06 cm) were generated. That the dispersed phases, the vessels, and the flow fields were all quite different in the two methods and that the sizes of the dispersed phases differed by one order of magnitude probably contributed to the small degree of systemic errors in Fig. 5. This discrepancy may be rectified by a correction factor based on two regression lines drawn through each method, but this approach does not completely eliminate the need to perform cumbersome photographic measurements.

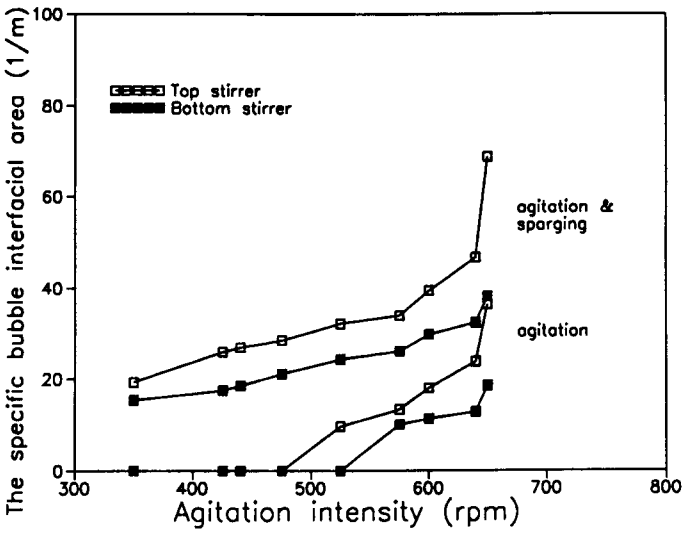

Fig. 6. Heterogeneity of the specific bubble interfacial area as measured by the optical probe at two fixed locations in an agitated fermentor: near the top stirrer (□) and the bottom stirrer (■). The stirred tank is operated at various stirrer speeds either with sparing (top two lines) or without sparging (bottom two lines).

Figure 6 shows the distribution of a measured by the optical probe around the top and bottom stirrers at various agitation intensities. In general, an increase in the agitation intensity led to an increase in the specific bubble interfacial area at both locations, with a consistently higher value for the top stirrer than the bottom stirrer under the same set of conditions. For agitation only without sparging (bottom two lines in Fig. 6), air entrainment from the medium surface started to be noticeable at ~525 rpm. At this stirrer speed, air was pulled into the top stirrer and broken up at the stirrer tip. As shown by the higher values of a for the top stirrer in Fig. 6, air dispersion was mostly localized at the top stirrer. Likewise, when the fermentor was operated with both agitation and air sparging (top two lines in Fig. 6), the drastic increase in a at 640~650 rpm was owing to the significant air entrainment from the medium surface.

The optical probe's upper detection range in a depends on the light path length. It is given approx by $al \leq 20$ (*13*). Thus, a shorter path length is needed to extend the effective upper limit. In actuality, because the fraction of transmitted light should be kept above 0.1 in order to achieve a reasonable degree of accuracy (*6*). The maximum value of a that the probe can reliably detect at the present light path length (0.055 m) is ~166 m^{-1}, which is about half of that calculated from $al \leq 20$. The lower range of a detectable by the present probe is indicated in Fig. 5 by the nonzero intercept of the calibration line with the horizontal axis. To extend the lower detection limit to a degree, the light path length should be increased, with a concomitant loss in the local resolution.

Although the current study focuses on a fermentor, other areas of application include reactor development and design, process scaleup, and mixing. In general, the present probe is well suited for measuring a in a nonscattering solution. However, appropriate corrections must be made if the probe is to be employed for on-line fermentation monitoring, if another phase (cells, oil droplets, solid substrates, and so on) is present and is changing over time, or if fouling is significant. Extending the optical probe to on-line applications is beyond the scope of this study.

CONCLUSION

An optical probe was constructed for monitoring the local specific bubble interfacial area in a fermentor. A mathematical calibration model that incorported probe-specific photoelectric characteristics was shown to be applicable to both systems employed to test the probe: uniform polystyrene spheres and nonuniform, nonspherical bubbles. Thus, probe calibration can be performed simply with polystyrene beads. The light transmission model was successful in translating the probe signal into a physical measurement of the specific interfacial area.

ACKNOWLEDGMENT

The authors would like to thank Richard V. Calabrese and Kuo-Ching Chang for the use of the macrophotographic system and the computerized photographic image processing facilities. This project is partially supported by a Biomedical Research Support Award (NIH Grant RR-07042) to NSW.

REFERENCES

1. Jones, O. C. and Delhaye, J. M. (1976), *Int. J. Multiphase Flow* **3,** 89.
2. Ishii, M. (1987), in *Multiphase Science & Technology,* vol. 3, Hewitt, G. F., Delhaye, J. M., and Zuber, N., eds., Hemisphere Pub. pp. 31–61.
3. Yang, J.-D. and Wang, N. S. (1991), *Biotechnol. Tech.* **5,** 349.
4. Vermeulen, T., Williams, G. M., and Langlois, G. E. (1955), *Chem. Eng. Prog.* **51,** 85F.
5. Calderbank, P. H. (1958), *Trans. Instn. Chem. Engrs.* **36,** 443.
6. McLaughlin, C. M. and Rushton, J. H. (1973), *AIChE J.* **19,** 817.
7. Hong, P. O. and Lee, J. M. (1983), *Ind. Eng. Chem. Process Des. Dev.* **22,** 130.
8. Bensler, H. P., Delhaye, J. M., and Favreau, C. (1987), in *ANS Proceedings,* National Heat Transfer Conference of ANS, pp. 240–246.
9. Bensler, H. P., Delhaye, J. M., and Favreau, C. (1991), in *Experimental Heat Transfer, Fluid Mechanics, and Thermodynamics,* Keffer, J. F., Shah, R. K., and Ganic, E. N., eds., Elsevier, pp. 1096–1104.

10. Horowitz, P. and Hill, W. (1980), *The Art of Electronics*, Cambridge University Press, Cambridge, England.
11. Chang, K.-C. (1990), *Analysis of Transient Drop Size Distributions in Dilute Agitated Liquid-Liquid Systems*, Ph.D. Thesis, University of Maryland, College Park, MD.
12. Chen, H. T. and Middleman, S. (1967), *AIChE J.* **13,** 989.
13. Lockett, M. J. and Safekourdi, A. A. (1977), *AIChE J.* **23,** 395.